



Cold-Set Gelation of Soybean and Amaranth Proteins by Hydration of Freeze-Dried Protein Previously Denatured in the Presence of Calcium

Anabella Marinacci¹ · Judith Piermaria¹ · Francisco Speroni¹

Received: 28 August 2023 / Accepted: 14 December 2023 / Published online: 28 December 2023
© The Author(s), under exclusive licence to Springer Science+Business Media, LLC, part of Springer Nature 2023

Abstract

The gelation of soybean and amaranth proteins through a three-step-strategy: heat-induced denaturation at low protein content (2 or 4 wt%) in the presence of calcium (0.075–0.250 mmol Ca/g protein) and at pH 7.0, followed by freeze drying, and rehydration at higher protein content (10 or 13 wt%) was evaluated for mixtures 80:20 (soybean:amaranth) and for soybean proteins alone. Gelation was favored by high protein contents during denaturation and rehydration, and by a Ca²⁺:protein ratio of 0.100 mmol Ca/g protein. Gels were soft (hardness from texture profile analysis was 0.26 N) and self-supporting and exhibited excellent water-holding capacity (99% upon centrifugation at 20,000xg). The aggregates formed during denaturation were weakly associated upon rehydration and were mostly extractable with water, which partially explained the softness of gels. The appropriate Ca²⁺:protein ratio would lead to a particular distribution of Ca²⁺ between free in solution and bound to proteins, which in turn balanced associations and repulsions allowing gelation. The presence of 20% amaranth proteins led to a more brownish color, a higher adhesiveness and a lower cohesiveness (texture), lower storage modulus, apparent viscosity, consistency index, and area of hysteresis (rheology) when compared to gels containing only soybean proteins. The mechanical differences suggest that soybean proteins dominated the three-dimensional matrix while amaranth proteins were less engaged and acted as a filler.

Keywords Cold-set gelation · Plant proteins · Water holding capacity · Self-supporting gels

Introduction

Many factors, such as health care or ideological reasons, play a role in consumers' food choices, driving new dietary trends towards increased consumption of plant-based proteins. In this context, soybean proteins have an important role since they provide a good balance in amino acid composition, their techno-functional properties are versatile and allow their incorporation in many foodstuffs, and they are available because of high levels of production and low cost [1, 2]. On the other hand, although amaranth proteins have agronomic advantages as they adapt to different soils and

climates and have various health benefits derived from their amino acid composition, bioactive peptides, and antioxidant polyphenols [3], their techno-functional properties are little known and therefore little used in the food industry. Amaranth proteins have a higher methionine content than soybean ones (which are limited in this essential amino acid) [4, 5], therefore they could be complemented to generate foods with high biological value and health-promoting compounds. The study of the techno-functional properties of amaranth proteins would favor their use as food ingredients, which would broaden the spectrum of vegetable protein sources.

Calcium is essential for healthy body functions and it is not easy to complete its necessary daily amount (ca. 1 g per day) [6]. The incorporation of calcium into preparations containing plant proteins is a challenge because calcium induces associations that under some conditions may improve techno-functional properties such as gelation, water holding capacity and viscosity, but under other conditions may lead to excessive aggregation, which in turn leads to a

✉ Francisco Speroni
franciscosperoni@gmail.com

¹ Centro de Investigación y Desarrollo en Criotecología de Alimentos (CIDCA) – CCT La Plata, Facultad de Ciencias Exactas, Universidad Nacional de La Plata (UNLP) and Consejo Nacional de Investigaciones Científicas y Técnicas (CONICET), Calle 47 and 116, La Plata, Argentina

decrease in protein solubility and the consequent worsening of those properties [7]. Therefore, a balance must be found between the attempt to incorporate a high dose of this essential nutrient and the need to keep the acceptability of the foods.

Hydrogels are viscoelastic systems that retain large amounts of water and provide texture to different foods. Gelation has been studied for soybean protein isolates (SPI) and amaranth protein isolates (API), SPI has shown excellent ability to gel under different conditions and with different strategies. API has not shown the same ability, its low solubility (compared to other plant globulins) may be a determining factor in forming gels with good characteristics, and genetic modifications have even been tried to improve the gelling capacity of amaranth proteins. [8–12]. The mixing of proteins can tune the properties of plant protein gels, which may lead to reinforcing, indifferent, or weakening effects compared to the theoretically expected properties. These effects depend on different phenomena, such as the dilution of the protein that dominates the formation of the network, the possibility of individual networks to coexist, the increase in the number of associative interactions, and/or the phase separation [13]. Protein aggregation and gelation occur simultaneously in heat-induced gelation [14]. Moreover, there is knowledge about the cold-set gelation of globular proteins, in which aggregation and gelation occur in a two-step sequence. The first step includes denaturation and aggregation of the proteins usually achieved by heat treatment, whereas gelation occurs in the second step upon changes in the composition of the medium [12, 15]. Piccini et al. [16] evaluated the possibility of obtaining gels from SPI through a three-step sequence: protein denaturation by high hydrostatic pressure or heating at low protein content (1 wt%) and in the presence of calcium (1.8 or 5.0 mM), freeze-drying, and finally rehydration at higher content (10 wt% protein). These authors obtained gels when high pressure induced the denaturation, but obtained insoluble aggregates when heating was the denaturation agent; possibly the different denaturation mechanisms led to different calcium-proteins interactions that require different calcium concentrations for gelation. Thus, it is interesting to evaluate other protein and calcium concentrations in the case of heating.

A protein gel forms because of a balance between repulsions and associations of polypeptides. The associations are hydrophobic interactions, hydrogen bonds, disulfide bridges, and coulomb forces between opposite electrical charges [17]. Among the latter, calcium bridges can link negatively charged amino acid residues and contribute to gel formation. The repulsive interactions are mainly electrostatic in nature and depend on the distance from the pH to the isoelectric point, the ζ -potential, the ionic strength, and the types of ions present. In the case of cold-set gels, some interactions are established in the first step,

which results in the formation of aggregates or structural units, meanwhile, other interactions are established in the last step and link those aggregates. The last step has a great dependence on electrostatic phenomena, thus pH changes or salts addition are done to reduce electrostatic repulsion and allow the approach of aggregates and the establishment of associations. Divalent ion salts are more effective in inducing gelation than monovalent ion salts because divalent cations can bind specifically to proteins [12]. Among calcium-induced interactions, the formation of calcium bridges needs a decrease in the energy barrier that allows the aggregates to approach one another and link, which can be achieved if charges are enough screened [14]. As an example, Maltais et al. [14] postulated that in gels obtained from soybean proteins, (pH 7, 8% protein content), calcium bridges contributed to the gel structure when the CaCl_2 concentration was 20 mM but not when it was 10 mM.

Two effects of calcium have been discriminated: a non-specific screening of electrostatic interactions by ions in solution (ionic strength), and a specific binding that reduces the effective charge density of the polypeptides [18]. The specific binding occurs through four main kinds of associations: interaction with carboxylate groups from glutamate and aspartate, calcium bridges that cross-link polypeptide chains, cation- π interaction with the deprotonated imidazole of histidine, and through weak cation-amide interaction with the carbonyl oxygen of exposed amide groups [19, 20]. This variety of interactions allows us to explain the effects of calcium on the gelation of soybean proteins, even at pHs lower than the isoelectric point [21], since calcium can bind to polypeptides even though the protein exhibits a net positive charge. Moreover, ions can exert effects on protein interactions and stability through an indirect mechanism by affecting the structure of water and competing for solvation with proteins, which generates stabilization and insolubilization (kosmotropic ions) or denaturation and solubilization (chaotropic ions). This effect is manifested in the Hofmeister or lyotropic series and mainly originated because of charge density. According to that series, calcium should unfold and solubilize soybean proteins, but it stabilizes and insolubilizes them [22]. It is possible that the lyotropic effect may not explain what happens with cations because the contribution due to their charge density (effect on water structure) is partially countered by the contribution of protein-cation-specific interactions. This phenomenon would be dominant at low salt concentrations, where interactions between cations and carboxylates are the most frequent [23]. These interactions coexist in equilibrium, therefore there are different conditions in which a fraction of calcium binds to certain degrees to the different protein sites while another fraction of calcium remains in solution and screens charges. Some of those conditions would favor the establishment of attractive

(such as calcium bridges and hydrogen bonds) and hydrophobic interactions that enough balanced with repulsions to generate a gel.

Taking into account the above, we hypothesize that no matter what procedure is used to denature, proper protein content and proper ratio of masses (and electrical charges) of calcium and plant proteins can be found and consequently gels could be obtained through the mentioned sequence (denaturation in the presence of calcium, freeze-drying, and rehydration). Since both SPI and API contain proteins with related structures, i.e. vicilins and legumins [24–26], it might be expected that once denatured simultaneously they can cross-link and modulate the mechanical properties of matrices. Either way, the addition of API would improve the biological value of SPI-based products and would increase the ingestion of healthy bioactive substances. If it works, this strategy would be the basis for generating foods with high nutritional value that are easy to prepare at home (the consumer should only add water) and also easy to swallow (which can be advantageous for elderly people or patients with certain diseases). The aim of this work was to evaluate the possibility of adding API to SPI to generate a dehydrated mixed product that gels upon the addition of water. In addition, testing the protein isolates separately will allow the evaluation of possible interactions in the ability to gel.

Materials and Methods

Materials

Soybeans were provided by a local market, La Plata, Argentina, and *Amaranthus hypochondriacus* grains were provided by Agronomy and Veterinary School of Rio Cuarto National University, Argentina. Calcium was incorporated as a CaCl_2 solution using $\text{CaCl}_2 \cdot 2\text{H}_2\text{O}$ (Sigma, USA). Bovine serum albumin was from Sigma (USA). All other chemicals were reagent grade.

Preparation of Protein Isolates

Amaranth grains and soybeans were ground and the resulting flours were sieved ($500\ \mu\text{m}$) prior to being defatted by exposure to hexane (ratio flour:hexane was 1:9) during 12 h at room temperature. Filtering was carried out by applying vacuum. The remaining solvent was evaporated at room temperature for 24 h.

Amaranth and soybean protein isolates were prepared according to Ventureira et al. [27] and to Manassero et al. [28], respectively. In both cases, a first step of alkaline protein extraction (pH 9.0 and 8.0 for API and SPI, respectively) was followed by an isoelectric precipitation step (pH 5.0 and 4.5 for API and SPI, respectively), protein isolates

were dispersed at pH 7.0 and freeze-dried. The Kjeldahl method [29] was applied to determine the protein content (N factors of 6.25 and 5.75 for SPI and API, respectively), which resulted in $92.9 \pm 0.6\%$ for SPI and $85.3 \pm 0.5\%$ for API (d.b.).

Protein Dispersions

Aqueous dispersions of 80:20 SPI:API mixtures, SPI and API were prepared at 2.0 or 4.0 wt%. Calcium chloride was added from a 1.0 M stock solution. The addition of calcium was done at different Calcium to protein ratios: 0.075; 0.100 or 0.250 mmol Ca^{2+} /g protein, which throughout the text are indicated without units for abbreviation. After calcium addition, the pH was corrected to 7.0 with 2 M NaOH.

Denaturing Treatment

Heat treatment was carried out by placing the samples in 50 mL centrifuge tubes, without internal stirring but shaking the tubes by hand every 5 min, in a thermostatic bath (Vicking, Argentina) at $95\ ^\circ\text{C}$ for 25 min, after which samples were freeze-dried. Protein content was determined by Kjeldahl method, no differences were found between the protein contents before and after heat treatment and freeze-drying.

ζ -potential

The ζ -potential was evaluated in dispersions of SPI:API mixtures that were heated at 4.0 wt% protein and then diluted with bi-distilled water up to 0.005 wt% protein. The samples with ratio 0.250 were filtered ($0.45\ \mu\text{m}$) to eliminate particles formed by insoluble protein. Measurements were carried out in a Nano ZS Zetasizer (Malvern Instruments Corp., Malvern, UK) in disposable polystyrene capillary cells with a light path of 10 mm at $25\ ^\circ\text{C}$.

Gel Formation Assays

Gel formation assays were carried out according to Piccini et al. [16]. Denatured and freeze-dried samples were dispersed in bi-distilled water at 10 or 13 wt%, stirred for 1 h, and centrifuged ($2,000\times g$, 1 min, $15\ ^\circ\text{C}$, Hermle, Z 326 K, Germany) to eliminate the foam. The foam was destabilized by acceleration; a residual foam, which occupied approximately 2% of the height of the tube at its top, was removed with a spatula and discarded. Samples were stored at $4\ ^\circ\text{C}$ for 24 h prior to demolding.

The samples were visually inspected for transparency, turbidity, or opacity, and for the ability to form self-supporting gels.

Characterization of Gels

Protein Extraction from Gels by Different Solvents

In order to evaluate the interactions that stabilized the gels, proteins were extracted with different solvents, with a method based on that from Peyrano et al. [30] with slight modifications. The solvents were water (for solubilizing unbound proteins); 0.4 M NaCl aqueous solution at pH 7.0; 0.05 M NaH₂PO₄ + 0.4 M NaCl at pH 7.0 (NaCl and NaCl in buffer interferes with electrostatic bonds); 0.05 M NaH₂PO₄ + 0.4 M NaCl + 6 M urea + 10 g/L SDS at pH 7.0 (urea and SDS interfere with hydrogen bonds and hydrophobic interactions); or 0.05 M NaH₂PO₄ + 0.4 M NaCl + 6 M urea + 10 g/L SDS + 5% β-mercaptoethanol at pH 7.0 (β-mercaptoethanol disrupts disulfide bonds) [30, 31]. Samples were dispersed at a 1:4 (gel:solvent) ratio and homogenized first with a vortex stirrer, then with a Thermomixer Eppendorf (750 rpm, 30 min, 30 °C), and finally again with a vortex stirrer. The samples that contained β-mercaptoethanol were heated at 100 °C for 5 min after the first vortex stirring. After homogenization, dispersions were centrifuged (10,000xg, 15 min, 4 °C) and the supernatants were stored at -80 °C until protein content analysis or molecular characterization by sodium dodecyl sulfate-polyacrylamide gel electrophoresis (SDS-PAGE).

Protein Extraction Levels The protein content of supernatants from the extraction from gels was determined by the Lowry method [32]. Bovine serum albumin was used as standard (0 to 1 mg/mL) and was solubilized in the different solvents that were used to extract proteins from gels. Absorbance was measured at 750 nm in a plate reader (Biotek Instruments, USA). The level of protein extraction was expressed as the percentage given by the protein in the supernatant relative to the total protein in the gel.

Molecular Characterization by SDS-PAGE Supernatants from gel extraction were analyzed by SDS-PAGE with a separating gel at 12 w/v% polyacrylamide and a stacking gel at 4% w/v polyacrylamide in a mini slabs system (BioRad Mini-Protean II). Gels composition, current and voltage conditions, fixation, and staining were as in Piccini et al. [16]. Low molecular weight markers in the range from 14.4 to 94 kDa (Pharmacia, Amersham, England) were used. Electrophoresis was carried out under non-reducing conditions, the only sample that was reduced was the one extracted with the buffer containing β-mercaptoethanol. In order to compare the levels of protein extraction, the samples corresponding to the extracts with different solvents were loaded using the same volume (10 μL), except for those containing β-mercaptoethanol in which half (5 μL) was used.

For this, all the extracts were previously diluted by mixing 200 μL of extract with 600 μL of water, subsequently, 600 μL of this dilution was added to 200 μL of electrophoresis sample buffer.

Rheological Characterization

Viscosity Flow behavior was determined at 20 °C in a Discovery HR20 rheometer (TA Instruments, USA) with a plate/plate geometry (40 mm diameter, 1 mm gap) through rotational tests by applying three flow stages: shear rate rising from 0 to 300 s⁻¹ in 90 s, holding for 1 min at 300 s⁻¹, and shear rate decreasing from 300 to 0 s⁻¹ in 90 s. The apparent viscosity was calculated in the up-curves at 51 s⁻¹. Flow and consistency index were determined by adjusting experimental results from down-curves with the Ostwald-de Waele model:

$$\tau = K (\dot{\gamma})^n$$

where τ is the shear stress (Pa), K is the consistency index, $\dot{\gamma}$ is the shear rate and n is flow index.

Viscoelasticity Small deformation oscillatory measurements were carried out at 20 °C in the same rheometer and with the same geometry probe. Measurements were carried out at a constant strain of 1%, which belonged to the linear viscoelastic region (previously determined at 1 Hz). Frequency sweeps were applied between 0.01 and 10.0 Hz to obtain the mechanical spectra (complex modulus, G^* , storage modulus, G' , and loss modulus, G'' , as a function of frequency). The G^* values versus angular frequency (ω) were modeled according to:

$$G^* = A \omega^{(1/z)}$$

Where A represents the structural strength of the gel and z is the number of rheological units interacting with one another in the three-dimensional network [33].

Texture Profile Analysis

Gels were prepared in cylindrical tubes (14 mm diameter), removed with the aid of a plunger, and cut to a height of 6 mm. The assays were carried out in CT3 Texture Analyzer (Brookfield Engineering Labs, USA) in compression mode. A plate-plate sensor system with a probe TA11/1000 at a constant rate of 0.5 mm/s was used. Gels were compressed (20% of their original height) in a two-cycle uniaxial test. Hardness, adhesiveness, springiness, and cohesiveness were obtained from the force-time curves according to Bourne [34].

Water Holding Capacity (WHC)

WHC was evaluated as in Piccini et al. [16] with different accelerations, portions of gels (0.75 g) were centrifuged (5,000, 10,000, 15,000, or 20,000 \times g, 15 min, 4 °C, Hermle, Z 326 K) in previously tared Eppendorf tubes. Supernatants were discarded and the residues were weighed. WHC was expressed as:

$$WHC = \frac{(W_0 - W_r)}{W_0} \times 100$$

where W_0 was the weight of water in the gel before centrifugation and W_r was the weight of water released upon centrifugation.

Color

The color parameters were measured on cylindrical gels lying on a white surface with Konica Minolta CR-400 (Japan) colorimeter. Results were expressed as L^* (lightness), a^* (redness/greenness), and b^* (yellowness/blueness) in the CIELab system.

Statistical Analysis

Assays were performed at least in triplicate. One-way analyses of variance were conducted. Differences between means were analyzed by Tukey's test at the significance level of $p < 0.05$. Statistical analysis was carried out using the Origin software (OriginLab Corporation, USA).

Results and Discussion

Gel Formation Assays

Different conditions of Ca:protein ratio and protein content during denaturation and rehydration were assayed in order to identify the conditions in which self-supporting gels could be obtained. Preliminary studies showed that API alone, unlike SPI alone, generated no self-supporting gels, but dispersions with low WHC in the ranges of protein contents assayed in this work (data not shown). Therefore, a low percentage (20%) of API was tested in the mixtures.

When the highest Ca:protein ratio (0.250) was applied for both protein contents (2 and 4 wt%), macroscopic particles (ca. 1–2 mm in diameter, observed with the naked eye) and insoluble aggregates (evidenced as turbidity) were formed during the heat treatment. Upon rehydration, these samples generated opaque systems that spontaneously released water, of which only the one denatured at 4 wt% and rehydrated at 13 wt% generated a weak self-supporting

gel. Macroscopic particles are not useful for gelling since they are too compact, interact with a small amount of water, so they precipitate quickly and generate a separate phase. On the other hand, some insoluble aggregates can interact with each other to gel and generate coarse systems with low WHC; while soluble aggregates generate ordered gels with high WHC [35]. Maltais et al. [14] suggested that high calcium concentrations increased the aggregates' size and the protein-protein associations, but decreased the protein-water associations, which resulted in a random ordering of the three-dimensional network.

At the lowest end of the range of Ca:protein ratio assessed (0.075), the rehydrated samples were turbid and with amber coloration, which indicated a lower degree of insolubilization than in samples with the highest ratio. Self-supporting gels with this Ca:protein ratio (0.075) were formed only when denaturation occurred at 4 wt% and rehydration was carried out at 13 wt%.

Samples with Ca:protein ratio of 0.100 were turbid and with amber coloration, the same as for the ratio of 0.075; self-supporting gels were obtained at this Ca:protein ratio when protein denaturation and rehydration were carried out at 2 and 13 wt%, respectively, and when protein denaturation was carried out at 4 wt%, for both protein contents assayed during rehydration. The gel obtained by denaturing at 4 wt% and rehydrating at 13 wt% was visually observed as the most structured since it better maintained its shape after demolding (Table 1).

These results indicate that the protein content during heat treatment affected the ability of the protein mixture to form self-supporting gels. At the highest protein content (4 wt%), more conditions were able to form these kinds of gels than at the lowest one (Table 1). Regarding protein content, Chen et al. [36] reported that the aggregate size formed from SPI at neutral pH during heating at 90 °C was higher as the protein content increased. Moreover, these authors stated that the gelation of SPI aggregates (evaluated at 20 °C) was favored by increasing aggregate size. Furthermore, Li et al. [37] reported that heat-induced aggregates from soybean proteins were larger the higher the protein content assayed, and that the percentage of the protein involved in the aggregates also increased with increasing protein content during heating. Thus, probably the aggregates formed in SPI:API mixture at 4 wt% were larger and more abundant than those obtained at 2 wt%; and the size and abundance of the aggregates, together with other structural characteristics, favored the establishment of interactions between them, which allowed the formation of self-supporting gels.

As was expected, the highest protein content during the rehydration favored the formation of a three-dimensional structure. This phenomenon was evidenced by the formation of self-supporting gels at both less favorable ratios (0.075 and 0.250) when protein content was 13 wt%.

Table 1 Formation of self-supporting gels and visual aspect of samples

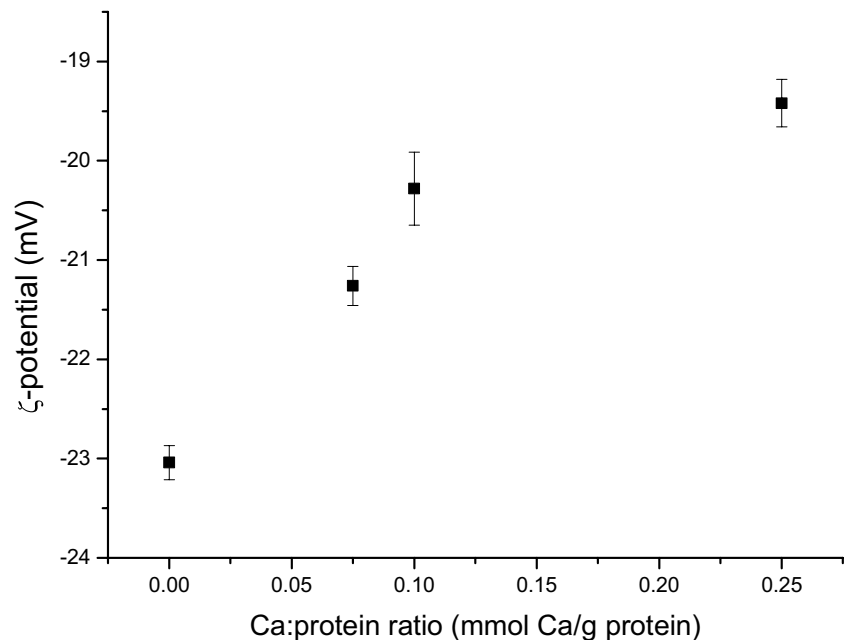
Protein content during denaturation (wt%)	Ca:protein ratio (mmol Ca ²⁺ to g protein)	Protein content during rehydration (wt%)	Formation of self-supporting gels	Visual aspect
2.0	0.075	10	-	amber turbid
		13	-	amber turbid
	0.100	10	-	amber turbid
		13	++	amber turbid
	0.250	10	-	ivory opaque
		13	-	ivory opaque
4.0	0.075	10	-	amber turbid
		13	++	amber turbid
	0.100	10	+	amber turbid
		13	+++	amber turbid
	0.250	10	-	ivory opaque
		13	+	ivory opaque

Conditions tested for mixtures of soybean and amaranth protein isolates (80:20)

Regarding Ca:protein ratio, most of the gels were obtained when it was 0.100. At the highest ratio (0.250) the samples showed a higher degree of insolubilization (opacity and phase separation). With the ratio of 0.250, it is likely that the calcium ions have reached a high degree of binding to protein and caused the charge shielding that led to aggregation and precipitation. Several researchers worked on the cold-set gelation of different protein systems (whey, β -lactoglobulin, SPI mixed with sorghum arabinoxylan, and tofu) and found that low calcium concentration promoted gelation and/or improved gel characteristics but excessive calcium

concentration avoided gelation or worsened the characteristics of gels [18, 38–40]. Regarding the mechanisms, Zheng et al. [41], studied heat-induced gelation of calcium-added SPI and reported that low calcium concentration promoted the establishment of hydrophobic interactions and hydrogen and ionic bonds, but at high calcium concentration, the protein insolubilization prevented the associative interactions. Taken together, our data and data from other researchers indicate that calcium-assisted gelation largely depends on the balance of the interactions of electrical charges that can be achieved with proper calcium content.

Fig. 1 ζ -potential of 0.005 wt% dispersions of soybean and amaranth protein isolates mixtures (80:20) as a function of Ca:protein ratio. Results are expressed as mean values \pm standard error. n was 5



ζ-Potential

The ζ-potential was measured in diluted protein dispersions of heat-treated SPI:API mixtures. The absolute value of ζ-potential decreased as the Ca:protein ratio increased (Fig. 1). A similar effect was reported by Manassero et al. [28] who worked with SPI alone. Since the samples had to be diluted to 0.005 wt% protein (and the sample with Ca:protein ratio of 0.250 was in addition filtered), it is possible that the ζ-potential values in the presence of calcium in the gels (13 wt% protein) were even closer to 0 mV. This effect would be due to the fact that when going from 13 mM CaCl₂ (in the gels at 13 wt% protein) to 0.005 mM CaCl₂ (in the dispersions to measure ζ-potential at 0.005 wt% protein) the balance between calcium bound to proteins and free calcium could move towards more free calcium. This fact was due to Le Chatelier's principle, with a dissociation degree that increases as total concentration decreases. These results suggest that the calcium-induced changes in ζ-potential would contribute to balancing the attractions and repulsions in order to form a gel. When the ζ-potential was more negative (Ca:protein ratio = 0.075), there could be a higher degree of electrostatic repulsion which could prevent the formation of the three-dimensional network. When the ζ-potential was closer to zero (Ca:protein ratio = 0.250) the proteins would exhibit a tendency to aggregate and precipitate due to an excessive decrease in electrostatic repulsion.

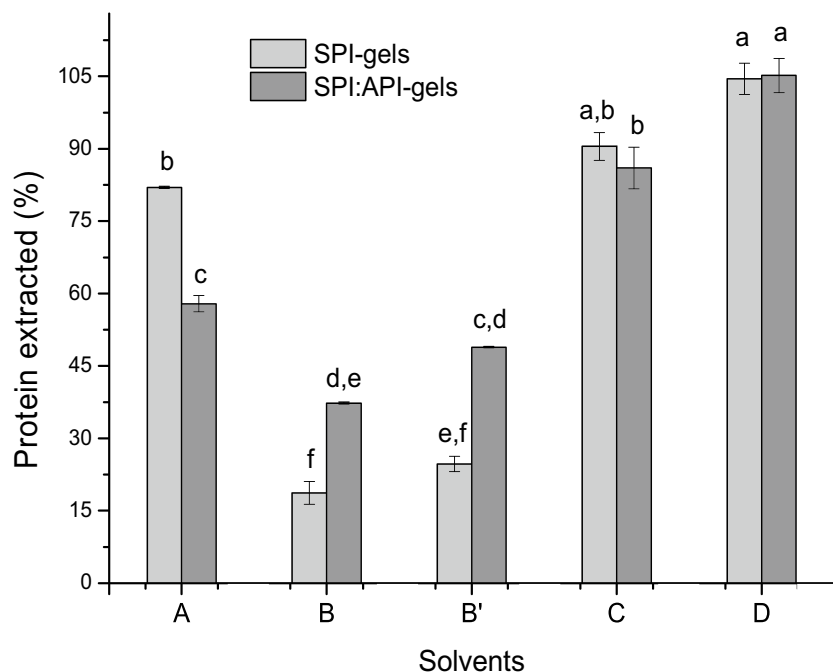
Taking into account these data, and that our objective was to obtain self-supporting gels, we decided to continue

the work characterizing the gels formed with a 0.100 Ca:protein ratio, denaturation at 4 wt% and rehydration at 13 wt%, with 80:20 SPI:API mixtures. Moreover, SPI alone was tested to compare and understand the effect of the protein mix.

Protein Extraction from Gels with Different Solvents

In order to understand the types of interactions that stabilize the microstructure, we analyzed the amount and nature of proteins that were extracted from the gels while exposed to different solvents. When the solvent is water, the soluble (and/or dispersible) unbound protein is extracted; whereas the protein involved in the matrix and the insoluble protein remain in the pellet after centrifugation. When the solvent has high ionic strength (in our case due to NaCl) the protein bound through electrostatic interactions is extracted; high ionic strength can also insolubilize a fraction of protein through the salting out effect, which promotes hydrophobic interactions that leads to aggregation [42, 43]. In the case of the solvent containing SDS and urea, hydrophobic interactions and hydrogen bonds are disassembled and the protein associated or insolubilized through those interactions is extracted [43]. The solvent with β-mercaptoethanol disrupts disulfide bonds, thus, protein associated through this covalent bond is released. The analysis must take into account that the protein extracted, depending on the interactions disrupted with each solvent, can be in individual form or involved in aggregates, which can be present in untreated protein isolates or, in our case, formed during the denaturation step.

Fig. 2 Protein extraction from SPI- and SPI:API-gels with different solvents. Solvent A: water. Solvent B: 0.4 M NaCl at pH 7. Solvent B': 0.05 M NaH₂PO₄ + 0.4 M NaCl at pH 7. Solvent C: 0.05 M NaH₂PO₄ + 0.4 M NaCl + 6 M urea + 1% SDS at pH 7. Solvent D: 0.05 M NaH₂PO₄ + 0.4 M NaCl + 6 M urea + 1% SDS + 5% β-mercaptoethanol at pH 7. Gels were obtained by denaturing at 4 wt%, with Ca:protein ratio of 0.1 mmol Ca/g protein and rehydrating at 13 wt%. Results are expressed as mean values ± standard error. Values with different letters indicate significant differences ($p < 0.05$)



Protein extracted with water was 58% for SPI:API-gels and 82% for SPI-gels (Fig. 2). This fact suggests that weak associations linked the most of the aggregates. The lower level of extraction in SPI:API gels could be caused by a higher fraction of insoluble protein in mixed gels. Possibly, in our samples, the dilution of CaCl_2 due to the addition of water (four parts of water for each part of gel for extraction assays) was enough to decrease the ionic strength and consequently increase the electrostatic repulsion and disassemble some bonds between aggregates. Kharlamova et al. [18] stated that the non-specific effect of charge screening was dependent on free Ca^{2+} concentration (ionic strength), whereas the reduction of the effective charge density of aggregates (ζ -potential) was dependent on Ca:protein ratio. This result suggests that in our gels, a fraction of calcium was attached to specific sites of protein meanwhile another fraction (and chloride ions) remained in solution and screened the remaining charges, which in turn allowed the approach of the aggregates and the establishment of few and/or weak associations between them. Regarding the aggregation degree of proteins in the gels, Ju and Kilara [44] studied the gelation of whey proteins and stated that the formation of heat-induced soluble aggregates was essential for cold-set gelation. In this sense, a high proportion of insoluble protein could negatively affect the ability to form gels, especially in the case of the SPI-API mixture, since API is very prone to become insolubilized upon heating [45]. The low solubility of API could partially explain the inability of API alone to form gel (Gel Formation Assays section).

When gels were exposed to a saline buffer or to a NaCl solution, a low amount of protein was extracted (even lower for SPI-gels than for SPI:API-gels). This fact could be due to a salting-out effect induced by NaCl, as was reported by Furukawa and Ohta [42] who observed that the solubility of heat-denatured (90 °C) SPI exhibited a low solubility in 0.5 M NaCl; the authors stated that the presence of salt favored the hydrophobic interactions leading to salting out. In the same way, low levels of protein extraction (6 and 13%) from tofu were also reported when solvents were 0.6 M NaCl solution or 20 mM Tris-HCl buffer at pH 8.0, respectively [46]. The high NaCl concentration interferes with electrostatic attractions such as calcium bridges, and also with electrostatic repulsion. Thus, NaCl has two opposite effects whose balance depends on the amounts of each type of interaction and influences the protein solubility. The low extraction levels observed in the presence of NaCl suggest that calcium bridges did not represent a great contribution to the stabilization of the gels. This fact would be in agreement with the results of Maltais et al. [14] who reported that calcium bridges require a high concentration of calcium; the authors stated that, in their experimental conditions, calcium bridges were formed at Ca:protein ratio of 0.250, but not when it was 0.125.

The extraction levels when the solvent included urea and SDS were 86% for SPI:API-gels and 91% for SPI-gels. These values indicate that a part of the associations inter- (and/or intra-) aggregates were hydrogen bonds and/or hydrophobic interactions, with a higher contribution in SPI-gels than in SPI:API-gels (the differences C-B and C-B' were higher for SPI- than for SPI:API-gels, Fig. 2). In this sense, Zhang et al. [47] reported that calcium, as a divalent cation, acts to shield negative charges on polypeptides and serves as a salt-bridge to enable polypeptide chains to approach one another; in this process, calcium favors the development of β -sheet structures to form SPI aggregates stabilized by hydrogen bonds: lastly, those aggregates could then be associated to form networks via hydrophobic interactions.

When extraction was carried out with the buffer that additionally contained β -mercaptoethanol, all of the protein was extracted from both types of gels, which indicates the presence of intra- and/or inter-aggregates disulfide bonds. The most of the disulfide bonds were probably intra-aggregate since aggregates stabilized by these covalent bonds are favored at high temperatures [48], in our case during heat treatment. The presence of inter-aggregate disulfide bonds established in the last step of gelation can not be ruled out (it was reported for cold-set gelation of whey proteins at acidic conditions [49]), but it would probably have resulted in a lower level of water extraction than that observed.

Molecular Characterization by SDS-PAGE

The bands generated by the polypeptides of untreated API and SPI can be observed in the corresponding lanes (Fig. 3). The untreated SPI exhibited bands corresponding to aggregates of a size that allowed them to enter the stacking gel but not the separating gel, and also others of size greater than 94 kDa. The bands corresponding to β -conglycinin polypeptides, i.e. α , α' , and β (72, 76, and 53 kDa, respectively) were detected. A very intense band corresponded to the AB subunit of glycinin (60 kDa). The glycinin A_3 polypeptide (42 kDa, a variant of A polypeptide that behaves differently than the other variants under some conditions [50]) appeared as a band of low intensity, whereas a band of 32 kDa and another corresponding to B polypeptide (and 20 kDa) had a higher intensity. This pattern of bands for SPI was similar to those reported by other authors such as Piccini et al. [16] and Song et al. [51]. The untreated API exhibited bands corresponded to aggregates higher than 94 kDa, but not so large that they could not enter the separating gel. The bands corresponding to AB subunits (56 and 54 kDa), A polypeptide (38 and 32 kDa), and B polypeptide (18 kDa) were detected. In addition, the 52 kDa polypeptide from the 7 S globulin, and its fragments of lower molecular weights were observed. This pattern of API was similar to those reported by Quiroga et al. [25, 26]. The bands corresponding to the amaranth proteins

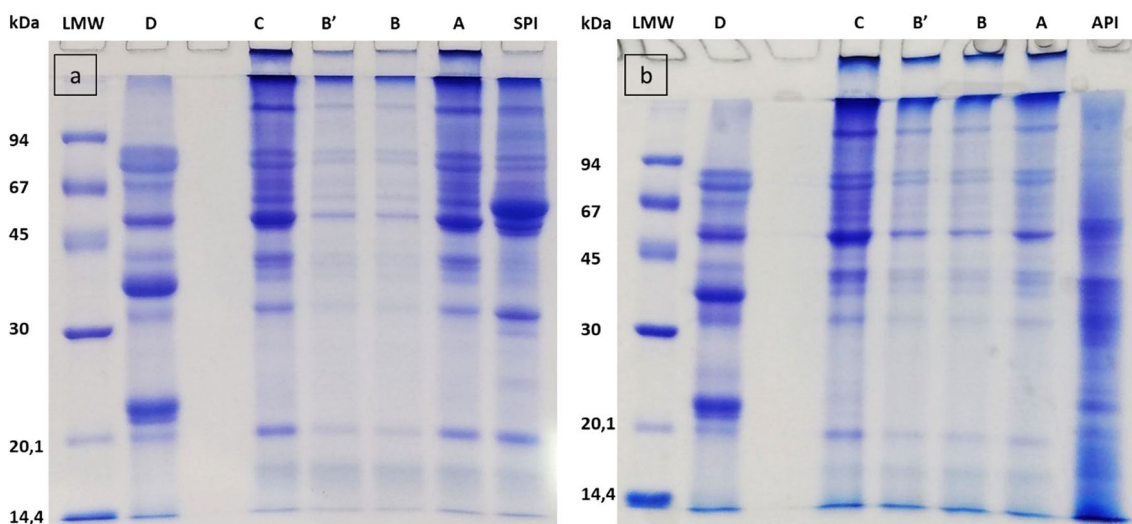


Fig. 3 SDS-PAGE of proteins extracted from SPI- (panel a) and SPI:API-gels (panel b) with different solvents. Lanes A: water. Lanes B: 0.4 M NaCl at pH 7. Lanes B': 0.05 M NaH_2PO_4 +0.4 M NaCl at pH 7. Lanes C: 0.05 M NaH_2PO_4 +0.4 M NaCl+6 M urea+1% SDS at pH 7. Lanes D: 0.05 M NaH_2PO_4 +0.4 M NaCl+6 M urea+1%

SDS+5% β -mercaptoethanol at pH 7. SPI: untreated soybean protein isolate. API: untreated amaranth protein isolate. LMW: low molecular weight standards. Gels were obtained from SPI (panel a) or SPI-API (panel b) by denaturing at 4 wt%, with Ca:protein ratio of 0.1 mmol Ca/g protein and rehydrating at 13 wt%

extracted from the SPI:API-gels were not distinguished from those of soybean because they had similar displacements, and consequently overlapped, and because of their lower content.

The proteins extracted with water (lanes A) exhibited more intense bands in the SPI-gels than in the SPI:API-gels, which was in accord with the highest level of water-extracted protein from SPI-gels (Fig. 2). Regarding the profiles of bands, the water-extracted proteins showed the same bands and with the same relative intensities as in the untreated SPI, with the exception of the appearance of aggregates so large that they did not enter the stacking gel, other aggregates that did not enter the separating gel, the glycinin A_3 polypeptide (42 kDa), and a relative decrease in the intensity of the AB subunit of glycinin. This fact suggests that heating in the presence of calcium induced the formation of high-molecular-weight aggregates that were not disassembled by the SDS present in the electrophoretic sample buffer and acrylamide gel; in addition, it suggests that glycinin was involved to a greater degree than β -conglycinin in their formation. Regarding the solubilized large aggregates, a similar behavior was reported by Piccini et al. [16], who made the same sequence of addition of calcium and heat treatment (1 wt% protein, Ca:protein ratio of 0.5) and stated that a fraction of the aggregates formed had very big sizes and were soluble. Otherwise, the glycinin A_3 polypeptide seems to behave differently from the other variants of A polypeptide when it participates in gels in the presence of calcium; in that sense, Zhao et al. [46] made tofu through a sequence that included two heatings and CaSO_4 incorporation between

the first and second heating and also showed that the glycinin A_3 polypeptide remained soluble.

When the proteins were extracted with NaCl solution or saline buffer (lanes B and B'), a similar profile as in the aqueous extraction was found for the most of bands, but with lower intensities. This phenomenon was due to the lower amount of protein, (the same volume was loaded, but the samples had lower solubility, Fig. 2). However, the intensities of the bands corresponding to aggregates that did not enter the stacking gel were lower in SPI- than in SPI:API-gels, which suggests that the higher level of protein extracted with NaCl from SPI:API-gels (Fig. 2) could have been at the cost of the solubilization of these aggregates. Moreover, the intensity of bands corresponding to the glycinin A_3 polypeptide was low, as in the untreated SPI.

In the cases of extraction with the buffer containing urea and SDS, solubilization was due to the disruption of intra-aggregate bonds, in addition to the inter-aggregates bonds. However, the relative intensities of bands in lanes C were indistinguishable from those obtained with water (lanes A). This similitude was due to the presence of SDS among electrophoresis reagents, which disassembled the hydrophobic interactions and hydrogen bonds that stabilized the water-extracted aggregates. It should be noted that although the profiles (intensity ratios in a lane) were similar for lanes A and C of both gels, the absolute intensities in SPI:API-gels, were lower in lane A than in lane C due to the lower level of protein extraction (Fig. 2).

The extracts obtained with the buffer that additionally contained β -mercaptoethanol (lanes D) were loaded with

half the volume of the other extracts. In these cases, the disappearance of large aggregates that were located at the top of stacking and separating gels was evidenced. This result indicates that disulfide bonds stabilized large aggregates that exhibited different molecular sizes. Moreover, the band corresponding to AB subunit disappeared with the consequent increase of intensity in the bands corresponding to polypeptides A₃ (42 KDa), A (37 KDa), and B (22 and 20 KDa).

Heat-induced aggregation of the glycinin AB subunit is due to sulfhydryl/disulfide interchange reactions [52]. Scilingo and Añón [53] stated that without heat treatment, specific calcium-soybean protein interactions existed, especially with glycinin. Taking into account these data, it is possible that a fraction of calcium has bound to proteins, especially to the AB subunit, then the heat treatment has denatured these calcium-protein complexes, and different aggregates mainly stabilized by disulfide bridges (and also by hydrogen bonds and hydrophobic interactions) were formed. The polypeptides from β-conglycinin would be aggregated through non-covalent interactions. Those aggregates would then associate through relatively weak or few interactions, favored by the screening provided by calcium, during rehydration to form the gels.

Rheological Characterization

Viscosity

Both samples exhibited pseudoplastic behavior during the shear rate rise and an overshoot at the start of this curve. The overshoot indicates a viscoelastic behavior given by a structure that was broken by the application of the shear stress. The pseudoplastic behavior is common in dispersions of macromolecules that can orient or deform in the direction of flow when subjected to tangential deformation; in our samples, it was more clearly observed during the shear rate descent (Fig. 4). Moreover, the presence of a hysteresis area was observed (Fig. 4). Fermented milk gels and yogurt presented similar performances [54]. The evaluation of the shear stress versus shear rate gradient in the performed mode can provide information that is well related to the appreciation that consumers may have during the initial handling of yogurt gels and during their consumption [55]. The SPI-gels were more viscous and had a greater area of hysteresis than SPI:API-gels (Table 2). The fit to the Ostwald-de Waele model carried out in the down-curves showed a higher consistency index, and a lower flow index for SPI samples than

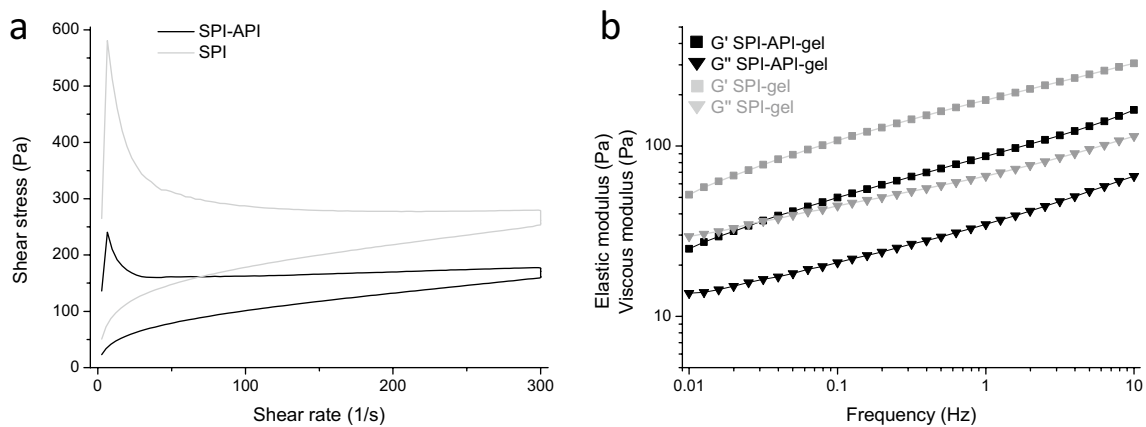


Fig. 4 Flow curves (panel a) and mechanical spectra (panel b) of SPI-API- and SPI-gels

Table 2 Rheological parameters

	Apparent viscosity at 51/s (Pa.s)	Area of hysteresis (Pa.s)	Consistency index (Pa.s ⁿ)	Flow index	G' at 1 Hz (Pa)	tan δ	Factor A (Pa.s/rad)	z
SPI:API	2.9 ± 0.2 ^b	14660.0 ± 1611.7 ^b	16.2 ± 0.8 ^b	0.386 ± 0.002 ^a	89.2 ± 19.0 ^b	0.40 ± 0.03 ^a	61.7 ± 16.9 ^b	3.8 ± 0.3 ^a
SPI	5.8 ± 0.4 ^a	29483.3 ± 2088.4 ^a	47.9 ± 4.0 ^a	0.292 ± 0.005 ^b	157.9 ± 24.9 ^a	0.38 ± 0.02 ^a	106.6 ± 19.0 ^a	4.2 ± 0.2 ^a

Results are expressed as mean values ± standard deviation. Values in the same column with different letters indicate significant differences (*p* < 0.05). *n* was 5 for flow curves, *n* was 3 for mechanical spectra

for SPI-API ones (Table 2). These data indicate a higher degree of structuring in SPI-gels than in the SPI:API-gels.

Viscoelasticity

In both types of gels and over the entire frequency range, the elastic behavior predominated over the viscous one. At 1 Hz, $\tan\delta$ was 0.40 and 0.38 for SPI:API- and SPI-gels, without a significant difference; however, the SPI-gels presented higher G' values than the SPI:API-gels (Table 2). The curves of G' as a function of frequency were almost parallel for SPI:API- and SPI-gels (Fig. 4). Taking into account the absolute values of G' and the value of $\tan\delta$ (Table 2), our data indicate that both samples were weak gels. The difference in G' values suggests that SPI-gels presented a greater number of attractive interactions than SPI:API-gels. The fact that the G' values have decreased with the addition of amaranth proteins, but that the $\tan\delta$ and the behavior of G' versus frequency have not changed suggests that the gel structure was the same and was made up or dominated by the soybean proteins that were in a lower content due to the incorporation of API. Possibly a high fraction of API was involved in insoluble aggregates (as it was proposed from the lower solubility in water of SPI:API-gels, Figs. 2 and 3) and acted as a filler with a low degree of association with the matrix. The proteins that are not engaged in the gel network do not contribute to the storage modulus of the gel [56]. To quantify this effect, G^* was modeled as a function of angular frequency, and the greatest strength was found in the SPI-gels (factor A, Table 2). Regarding z , the values fell into the range reported for yogurt and jams [57]; a trend was observed (the difference was not significant) towards a greater number of interactions in the SPI-gels (Table 2). Although the model is very simple and has questionable assumptions [57], it gives a link between continuum and macroscopic features of weak gels and showed a trend that was consistent with the idea that API did not interact much with SPI, but rather acted as a filler. This result contradicted our hypothesis that certain structural characteristics shared by amaranth and soybean proteins could facilitate the formation of a mixed network.

Texture Profile Analysis

Table 3 shows the parameters of texture profile analysis of the gels obtained from SPI or SPI:API. The hardness values of SPI:API- and SPI-gels were similar. These values were similar to those found by Yang et al. [58], who reported a hardness of approximately 0.2 N for cold-set gels obtained from 10% SPI by lactic acid acidification. However, other authors reported higher hardness values (3 N) for gels formed from amaranth protein isolate, 15 wt% protein, by heat treatment at 95 °C [8]. Tofu, a soybean-based food

matrix with a protein content of 7.3%, obtained by two heating steps at 90 °C and the use of CaSO_4 showed a hardness of 3.1 N [46]. These data indicate that the textural characteristics of gels depend largely on the processing conditions and that heat-induced gels are often harder than cold-set ones. Regarding the intermolecular forces, the hardness depends on the number and type of bonds between the polypeptides. In our samples, the strongest interactions, such as disulfide bridges, were established during heating at low protein content (4 wt%) [59], which generated individual aggregates. The associations between aggregates were established upon rehydration at 13 wt% and were weak since many of them could be broken down with water (Fig. 2) and led to low values of hardness. Thus, most of the large aggregates that appeared among the water-extracted protein and were stabilized by disulfide bonds (lanes A and D of Fig. 3) were probably formed during heating. Thus, our gels had a heterogeneous distribution of interactions since the strongest ones would be intra-aggregates, while weak interactions would be inter-aggregates, which would explain why, despite the high protein content, the gels were softer than other SPI- or API-based gels. It is possible that the difference in the number of interactions postulated from the small deformation rheology tests (Table 2) has not manifested itself as a difference in the hardness values due to a lower sensitivity of the texturometer for gels of this type, and also because the

Table 3 Textural parameters

	Hardness (N)	Cohesiveness	Adhesiveness (N.mm)	Springiness
SPI:API	0.25 ± 0.02 ^a	0.93 ± 0.08 ^b	0.43 ± 0.12 ^a	1.25 ± 0.08 ^a
SPI	0.26 ± 0.05 ^a	1.01 ± 0.04 ^a	0.24 ± 0.12 ^b	1.19 ± 0.15 ^a

Results are expressed as mean values ± standard deviation. Values in the same column with different letters indicate significant differences ($p < 0.05$). n was 9

texture test causes greater deformation and can even break down part of the structure.

The value of cohesiveness was nearly 1, which suggests that the gels were deformed during the first compression but bonds quickly re-established and recovered the matrix. This result seems unexpected if one takes into account the hypothesis that the associations between aggregates were weak. The value of this parameter was slightly but statistically lower for SPI:API-gels than for SPI ones, which suggests that the attractive interactions between aggregates were more numerous in SPI-gels. This finding could be explained as the effect of insoluble aggregates of API that were present as a filler that decreased the content of the cross-linked soybean proteins, as was postulated in “Viscoelasticity” section (difference in G' values, Fig. 4; Table 2).

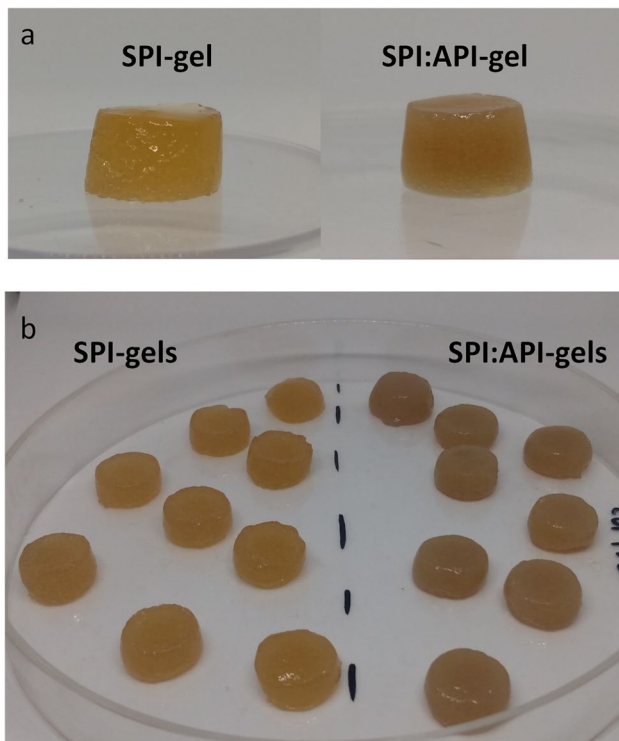


Fig. 5 SPI- and SPI:API-gels. Recently demolded (panel a). After texture profile analysis (panel b)

Adhesiveness corresponds to the work required to overcome the attractive forces between the surface of the material and other materials [60]. Both gels were adhesive, the highest value of adhesivity was found for SPI:API-gels. Adhesion can be described as the sum of two contributions: surface energy (type and strength of bonding) and cohesive energy (viscoelastic and plastic deformation within the adhesive) [61]. In that sense, an inverse correlation between G' and adhesiveness was reported [61]. It is possible that our gels have a similar behavior, in which the lower G' values of SPI-API gels led to enhanced adhesiveness.

The springiness was greater than 1 for both gels. Considering that the gels were adhesive and soft, it is likely that the springiness values higher than 1 correspond to a stretching of the gel due to its adhesion to the probe. The shape of both types of gels was well maintained after analysis, with the top edge becoming blunter (Fig. 5), which can be related to the high values of springiness and cohesiveness.

Water Holding Capacity

WHC was assessed by difference of weight after centrifuging, we tried to use low accelerations to disturb the gel structure as little as possible, but no water was released in the range 5,000–15,000 g . Therefore, the values of Table 4 correspond to centrifugation at 20,000 g . Thus,

Table 4 Water holding capacity and color parameters of gels in the CIELab system

	Water holding capacity (%)	L*	a*	b*
SPI:API	99.1 ± 0.7 ^a	47.9 ± 1.0 ^a	0.7 ± 0.4 ^a	10.1 ± 1.1 ^a
SPI	98.5 ± 0.6 ^a	48.1 ± 2.0 ^a	2.7 ± 0.3 ^b	16.4 ± 2.0 ^b

L*: Lightness. a*: redness/greenness. b*: yellowness/blueness

Results are expressed as mean values ± standard deviation. Values in the same column with different letters indicate significant differences ($p < 0.05$). n was 3 for water holding capacity. n was 5 for color measurements

the gels formed from SPI and SPI:API upon this three-step strategy exhibit excellent WHC. The WHC values were almost 100% when samples were centrifuged at very high acceleration and were higher than those reported by other authors who worked with cold-set gelation of calcium-added SPI at Ca:protein ratios of 0.11 [11] or 0.10 [62]. Peyrano et al. [63] made heat-induced gels from calcium-added cowpea proteins and found WHC values from 20% (ratio 0.53) to 82% (ratio 0.13); the low WHC values with increasing Ca:protein ratio were explained as the effect of calcium favoring protein-protein interactions at the expense of protein-water ones.

The WHC capacity depends on protein-water interactions and on capillarity. Brito-Oliveira et al. [62] stated that gels made-up from disordered aggregates are porous and that matrices with dilated pores tend to inhibit the extent of immobilization of water through capillary forces. Taking into account that a large amount of protein was extracted with water (Fig. 2) and that the gels with Ca:protein ratio of 0.100 were cloudy but not opaque (as were the dispersions with ratio of 0.250, Table 1), we concluded that our gels were formed in part by soluble aggregates and in part by insoluble aggregates that together had a high affinity for water and/or that generated small interstices that contributed to the WHC through capillarity.

Color

The color of gels originates in part from the intrinsic color of the protein isolates (due to their chemical composition); another contribution to their appearance comes from the presence of insoluble protein, which in turn modulates the microstructure of the gel [35]. The color parameters are shown in Table 4. The SPI-gels presented an amber and cloudy appearance while the SPI:API-gels presented an amber color that was cloudier, this cloudiness was due to the presence of insoluble aggregates [15] that probably were more abundant in SPI:API-gels. The gels obtained by Piccini et al. [16] through the same sequence as in this work, but

denaturing with high hydrostatic pressure were translucent at a Ca:protein ratio of 0.18, which was explained by the high solubility of aggregates. Positive values of a^* and b^* indicate that the samples have a tendency towards red and yellow coloration, respectively. The lower values of a^* and b^* in the SPI:API gels agree with the more neutral color (brown) of these gels perceived by the eye (Fig. 5). This difference may be due to a higher content of polyphenols associated with amaranth proteins [64].

Conclusions

Relatively soft, self-supporting gels with excellent WHC could be formed from SPI:API (80:20) and SPI through a sequence consisting of the addition of calcium to a dispersion at low protein content, heat-induced denaturation, freeze-drying, and rehydration at higher protein and calcium contents. Although the heat-induced aggregates were stabilized by strong bonds such as disulfide bridges, the inter-aggregate bonds established during rehydration were relatively weak or few in number. Most of the inter-aggregate interactions appeared to be mediated or allowed by the non-specific charge screening effect of divalent ions since the mere dilution with water caused more than half of the protein to be released from the gel matrix. These phenomena explained why the gels were soft despite their high protein content. Among the interactions, electrostatic attractions (such as calcium bridges) did not seem to have been relevant in setting the gels. The Ca:protein ratio and the protein contents during denaturation and rehydration were very important factors in the formation of the gels. The presence of 20% amaranth proteins generated gels with a more brownish color and a lower degree of structuration, which was reflected as differences in the values of rheological and textural parameters. Possibly the SPI dominated the network and the incorporation of API decreased the content of the network-forming proteins while acting as a filler composed of insoluble amaranth proteins.

Since there was no phase separation during or after heating in the presence of calcium (at 4 wt% protein), and the samples were cloudy, we consider that for cold-set gelation of these plant storage proteins, the aggregates formed during heating can be a mixture of soluble and insoluble (but colloidal stable) species. Moreover, the possibility of forming a cold-set gel depends largely on the balance between electrostatic repulsions and attractions. This balance depended on ζ -potential and ionic strength and should be very close to the precipitation condition, but not reach it.

This work raises questions about the different gelling abilities of soybean and amaranth proteins, about the

existence of optimal ratios between these proteins, and between calcium and protein contents, and about the possibility of the formation of mixed aggregates (under other experimental conditions) and their effect in gelation, future research may clarify these concerns.

This system could be the basis for easily prepared and consumable foods, for example for dysphagia patients or elderly people, who need highly nutritive and easy-to-eat foodstuff that could be either soft solids or thickened liquids.

Acknowledgements The authors wish to thank María Fernanda Hamet for her kind and thorough technical assistance.

Author Contributions A.M.: Methodology, Validation, Formal analysis, Investigation, Data Curation, J.P.: Conceptualization, Methodology, Investigation, Resources, Data Curation, Writing – Review & Editing, Supervision, Funding acquisition F.S.: Conceptualization, Methodology, Investigation, Project administration, Data Curation, Writing – Review & Editing, Supervision, Funding acquisition.

Funding This work was supported by the CONICET (PIP 2021–2023 1147).

Data Availability The data that support the findings of this study are available from the corresponding author [FS], upon reasonable request.

Declarations

Competing Interests The authors declare no competing interests.

References

1. K. Nishinari, Y. Fang, S. Guo, G.O. Phillips, *Food Hydrocoll.* (2014). <https://doi.org/10.1016/j.foodhyd.2014.01.013>
2. M.M. García de Oliveira, K. de Souza, M.A. Mauro, *Food Biophys.* (2021). <https://doi.org/10.1007/s11483-020-09659-3>
3. A.E. Nardo, S. Suárez, A.V. Quiroga, M.C. Añón, *Front. Plant Sci.* (2020). <https://doi.org/10.3389/fpls.2020.578631>
4. S. Gorinstein, E. Pawelzik, E. Delgado-Licon, R. Haruenkit, M. Weisz, S. Trakhtenberg, *J. Sci. Food Agric.* (2002). <https://doi.org/10.1002/jsfa.1120>
5. P. Qin, T. Wang, Y. Luo, *J. Agric. Food Res.* (2022). <https://doi.org/10.1016/j.jafr.2021.100265>
6. Institute of Medicine (US) Committee to Review Dietary Reference Intakes for Vitamin D and Calcium, *Dietary Reference Intakes for Calcium and Vitamin D*, ed. by A.C. Ross, C.L. Taylor, A.L. Yaktine, H.B. Del Valle (National Academies Press (US), 2011)
7. Y. Peng, K. Kyriakopoulou, J.K. Keppler, P. Venema, A.J. van der Goot, *Food Hydrocoll.* (2022). <https://doi.org/10.1016/j.foodhyd.2021.107191>
8. M.V. Avanza, M.C. Puppo, M.C. Añón, *Food Hydrocoll.* (2005). <https://doi.org/10.1016/j.foodhyd.2004.12.002>
9. K. Shevkani, N. Singh, J.C. Rana, A. Kaur, *Int. J. Food Sci. Technol.* (2014). <https://doi.org/10.1111/ijfs.12335>
10. T. Nicolai, C. Chassenieux, *Curr. Opin. Food Sci.* (2019). <https://doi.org/10.1016/j.cofs.2019.04.005>
11. A. Maltais, G.E. Remondetto, R. Gonzalez, M. Subirade, *J. Food Science: Food Chem. Toxicol.* (2005). <https://doi.org/10.1111/j.1365-2621.2005.tb09023.x>

12. L. Carrasco-Peña, L.A. Osuna-Castro, A. De León Rodríguez, N. Maruyama, J.F. Toro-Vazquez, J.A. Morales-Rueda, Barba De La Rosa, J. Agric. Food Chem. (2013). <https://doi.org/10.1021/jf3050999>
13. S. Guidi, F.A. Formica, C. Denkel, Food Res. Int. (2022). <https://doi.org/10.1016/j.foodres.2022.111752>
14. A. Maltais, G.E. Remondetto, M. Subirade, Food Hydrocoll. (2008). <https://doi.org/10.1016/j.foodhyd.2007.01.026>
15. A.A. Hugo, P.F. Pérez, M.C. Añón, F. Speroni, Food Hydrocoll. (2014). <https://doi.org/10.1016/j.foodhyd.2013.10.025>
16. L. Piccini, A. Scilingo, F. Speroni, F Biophysics. (2019). <https://doi.org/10.1007/s11483-018-9558-z>
17. M. Corredig, in *Ingredient Interactions Effects on Food Quality*, ed. by A.G. Gaonkar, A. McPherson (Taylor & Francis, 2006), p. 283
18. A. Kharlamova, T. Nicolai, C. Chassenieux, Food Res. Int. (2018). <https://doi.org/10.1016/j.foodhyd.2017.11.049>
19. R.D. Kroll, Cereal Chem. **61**, 490 (1984)
20. I. Asakereh, K. Lee, O.A. Francisco, M. Khajehpour, ChemPhysChem (2022). <https://doi.org/10.1002/cphc.202100884>
21. M.C. Puppo, M.C. Añón, Food Hydrocoll. (1999) [https://doi.org/10.1016/S0268-005X\(98\)00079-4](https://doi.org/10.1016/S0268-005X(98)00079-4)
22. F. Speroni, M.C. Añón, M. de Lamballerie, Food Res. Int. (2010). <https://doi.org/10.1016/j.foodres.2010.03.022>
23. M. Boström, F.W. Tavares, S. Finet, A. Skouri-Paneta, A. Tardieu, B.W. Ninham, Biophys. Chem. (2005). <https://doi.org/10.1016/j.bpc.2005.05.010>
24. E. Derbyshire, D.J. Wright, D. Boulter, Phytochemistry (1976). [https://doi.org/10.1016/S0031-9422\(00\)89046-9](https://doi.org/10.1016/S0031-9422(00)89046-9)
25. A. Quiroga, E.N. Martínez, H. Rogniaux, A. Geairon, M.C. Añón, Protein J. (2009). <https://doi.org/10.1007/s10930-009-9214-z>
26. A. Quiroga, E.N. Martínez, H. Rogniaux, A. Geairon, M.C. Añón, J. Agric. Food Chem. (2010). <https://doi.org/10.1021/jf103296n>
27. J.L. Ventureira, A.J. Bolontrade, F. Speroni, E. David-Briand, A. Scilingo, M.H. Ropers, F. Boury, M.C. Añón, M. Anton, LWT (2012). <https://doi.org/10.1016/j.lwt.2011.07.024>
28. C.A. Manassero, E. David-Briand, S.R. Vaudagna, M. Anton, F. Speroni, Food Bioprocess Technol. (2018). <https://doi.org/10.1007/s11947-018-2084-7>
29. AOAC, *Official methods of analysis*, 15th edn. (Association of Official Analytical Chemists, Washington, 1990)
30. F. Peyrano, M. de Lamballerie, M.V. Avanza, F. Speroni, Food Hydrocoll. (2021). <https://doi.org/10.1016/j.foodhyd.2020.106191>
31. X.D. Sun, S.D. Arntfield, Food Hydrocoll. (2012). <https://doi.org/10.1016/j.foodhyd.2011.12.014>
32. O.H. Lowry, N.J. Rosebrough, L.A. Farr, R.J. Randall, J. Biol. Chem. (1951). [https://doi.org/10.1016/s0021-9258\(19\)52451-6](https://doi.org/10.1016/s0021-9258(19)52451-6)
33. T.G. Mezger, *The Rheology Handbook*, 5th edn. (Vincentz Network GmbH & Co. KG, Hanover, 2020), pp. 198–199
34. M.C. Bourne, Food Technol. **32**, 62–66 (1978)
35. A.M. Hermansson, J. Am. Oil Chem. Soc. (1986). <https://doi.org/10.1007/BF02638232>
36. N. Chen, C. Chassenieux, T. Nicolai, Food Res. Int. (2018). <https://doi.org/10.1016/j.foodhyd.2017.09.021>
37. X. Li, Y. Li, Y. Hua, A. Qiu, C. Yang, S. Cui, Food Chem. (2007). <https://doi.org/10.1016/j.foodchem.2007.02.003>
38. T. Phan-Xuan, D. Durand, T. Nicolai, L. Donato, C. Schmitt, L. Bovetto, Food Hydrocoll. (2014). <https://doi.org/10.1016/j.foodhyd.2012.09.008>
39. J. Yan, L. Yin, Y. Qu, Y. Wenjia, M. Zhang, J. Su, X. Jia, Food Hydrocoll. (2022). <https://doi.org/10.1016/j.foodhyd.2022.107997>
40. X. Wang, M. Zeng, F. Qin, B. Adhikari, Z. He, J. Chen, Food Chem. (2018). <https://doi.org/10.1016/j.foodchem.2017.09.044>
41. L. Zheng, F. Teng, N. Wang, X.N. Zhang, J.M. Regenstein, J.S. Liu, Y. Li, Z.J. Wang, Appl. Sci. (Switzerland) (2019). <https://doi.org/10.3390/app9061076>
42. T. Furukawa, S. Ohta, Agric. Biol. Chem. (1983). <https://doi.org/10.1271/bbb1961.47.751>
43. M.C. Puppo, C.E. Lupano, M.C. Añón, J. Agric. Food Chem. (1995). <https://doi.org/10.1021/jf00057a008>
44. Z.Y. Ju, A. Kilara, J. Food Sci. (1998). <https://doi.org/10.1111/j.1365-2621.1998.tb15728.x>
45. M.V. Avanza, M.C. Añón, J. Sci. Food Agric. (2007). <https://doi.org/10.1002/jsfa.2751>
46. H. Zhao, W. Li, F. Qin, J. Chen, Int. J. Food Sci. Technol. (2016). <https://doi.org/10.1111/ijfs.13010>
47. J. Zhang, L. Liang, Z. Tian, L. Che, M. Subirade, Food Chem. (2012). <https://doi.org/10.1016/j.foodchem.2012.01.049>
48. K. Shimada, J.C. Cheftel, J. Agric. Food Chem. (1988). <https://doi.org/10.1021/jf00079a038>
49. A.C. Altung, R.J. Hamer, C.G. de Kruijff, R.W. Visschers, J. Agric. Food Chem. (2000). <https://doi.org/10.1021/jf000474h>
50. N. Maruyama, T. Fukuda, S. Saka, N. Inui, J. Kotoh, M. Miyagawa, M. Hayashi, M. Sawada, T. Moriyama, S. Utsumi, Pytochemistry (2003). [https://doi.org/10.1016/s0031-9422\(03\)00385-6](https://doi.org/10.1016/s0031-9422(03)00385-6)
51. B. Song, N.W. Oehrle, S. Liu, H.B. Krishnan, J. Agric. Food Chem. (2016). <https://doi.org/10.1021/acs.jafc.6b03677>
52. S. Petruccelli, M.C. Añón, J. Agric. Food Chem. (1995). <https://doi.org/10.1021/jf00060a009>
53. A.A. Scilingo, M.C. Añón, J. Am. Oil Chemists' Soc. (2004). <https://doi.org/10.1007/s11746-004-0858-y>
54. M.F. Hamet, J.A. Piermaria, A.G. Abraham, LWT Food Sci. Technol. (2015). <https://doi.org/10.1016/j.lwt.2015.03.097>
55. D.M. Folkenberg, P. Dejmeck, A. Skriver, H. Skov Guldager, R. Ipsen, Int. Dairy J. (2006). <https://doi.org/10.1016/j.idairyj.2004.10.013>
56. C. Wu, T. Wang, C. Ren, W. Ma, D. Wu, X. Xu, L.S. Wang, M. Du, Compr. Rev. Food Sci. Food Saf. (2018). <https://doi.org/10.1111/1541-4337.12682>
57. D. Gabrielle, B. de Cindio, P. D'Antona, Rheol. Acta (2001). <https://doi.org/10.1007/s003970000139>
58. X. Yang, C. Ke, L. Li, J. Food Eng. (2021). <https://doi.org/10.1016/j.jfoodeng.2020.110243>
59. S. Petruccelli, M.C. Añón, J. Agric. Food Chem. (1995). <https://doi.org/10.1021/jf00055a004>
60. M.V. Chandra, B.A. Shamasundar, Int. J. Food Prop. (2014). <https://doi.org/10.1080/10942912.2013.845787>
61. B.J. Dobraszczyk, J. Texture Stud. (1997). <https://doi.org/10.1111/j.1745-4603.1997.tb00108.x>
62. T.C. Brito-Oliveira, M. Bispo, I.C.F. Moraes, O.H. Campanella, S.C. De Pinho, Food Biophys. (2018). <https://doi.org/10.1007/s11483-018-9529-4>
63. F. Peyrano, M. de Lamballerie, M.V. Avanza, F. Speroni, Food Hydrocoll. (2022). <https://doi.org/10.1016/j.foodhyd.2021.107220>
64. S.H. Guzmán-Maldonado & O. Paredes-López, in *Functional foods: biochemical and processing aspects* ed. by G. Mazza, (C.R.S. Press, 1998), p. 293

Publisher's Note Springer Nature remains neutral with regard to jurisdictional claims in published maps and institutional affiliations.

Springer Nature or its licensor (e.g. a society or other partner) holds exclusive rights to this article under a publishing agreement with the author(s) or other rightsholder(s); author self-archiving of the accepted manuscript version of this article is solely governed by the terms of such publishing agreement and applicable law.